

ARTICLE

# Vacuum Filling Simulation with Combined Lagranian and VOF Method

Yujia Chen Maoxuan Cai Shixun Zhang  Na Zhang  Wei Cao\* 

National Engineering Research Center for Advanced Polymer Processing Technology, Zhengzhou University, Zhengzhou, Hennan, 450002, China

ARTICLE INFO

*Article history*

Received: 30 December 2021

Revised: 28 February 2022

Accepted: 21 March 2022

Published Online: 30 March 2022

*Keywords:*

Vacuum

Finite element method

Lagranian technique

VOF method

Flow front

ABSTRACT

Jetting succeeded by accumulation is the characteristic of the vacuum filling, which is different from the conventional pressure-driven flow. In order to simulate this kind of flow, a three-dimensional theoretical model in terms of incompressible and viscous flow is established, and an iterative method combined with finite element method (FEM) is proposed to solve the flow problem. The Lagranian-VOF method is constructed to trace the jetting and accumulated flow fronts. Based on the proposed model and algorithm, a simulation program is developed to predict the velocity, pressure, temperature, and advancement progress. To validate the model and algorithm, a visual experimental equipment for vacuum filling is designed and constructed. The vacuum filling experiments with different viscous materials and negative pressures were conducted and compared with the corresponding simulations. The results show the flow front shape closely depends on the fluid viscosity and less relates to the vacuum pressure.

## 1. Introduction

Vacuum filling is an approach that uses vacuum to suck materials to fill the cavity. It is widely used in vacuum-assisted resin transfer molding (VARTM) and vacuum infusion molding process (VIMP). The most difficult issue is the prediction of complete fill time which closely depends

on the fluid viscosity, density and vacuum. In order to simulate the process, scientists and engineers have developed some models and numerical methods to trace the flow advancement, calculate the values of physical variables and predict the filling time<sup>[1]</sup>.

Using numerical simulation can predict the development and evolution of the flow front during the filling

\*Corresponding Author:

Wei Cao,

National Engineering Research Center for Advanced Polymer Processing Technology, Zhengzhou University, Zhengzhou, Hennan, 450002, China;

Email: [wcao@zzu.edu.cn](mailto:wcao@zzu.edu.cn)

DOI: <https://doi.org/10.30564/jmmmr.v5i1.4511>

Copyright © 2022 by the author(s). Published by Bilingual Publishing Co. This is an open access article under the Creative Commons Attribution-NonCommercial 4.0 International (CC BY-NC 4.0) License. (<https://creativecommons.org/licenses/by-nc/4.0/>).

process, optimize the process and mold structure of composite molding<sup>[2]</sup>, and improve the quality of parts<sup>[3,4]</sup>. Song and Youn<sup>[5]</sup> established an analytical model for the post-infusion VARTM process by the non-rigid control volume approach. They successfully predicted the thickness gradient due to the flexible nature of the bagging approach and the pressure gradient developed during infusion. It has also been used to predict the resin bleeding behavior for various processing scenarios. Robinson and Kosmatka<sup>[6]</sup> established compaction and permeability constitutive models, and proposed a numerical method to simulate the post-filling. Yang et al.<sup>[7]</sup> built the resin flow governing equations for vacuum-assisted resin infusion and an approach to calculate the primary flow by the normal Darcy's law. They conducted three examples to verify the precision and flexibility of the approach. Regarding resin as an incompressible fluid, Cai et al.<sup>[8]</sup> also used Darcy's law to describe the position of the resin flow front in the mold and the filling time, and used RTM-worx to complete the flow filling simulation.

There are two types of methods for advancement tracking, which are classified as Lagrangian and Eulerian<sup>[9]</sup>. The two methods are based on the strategies of mobile mesh and fixed mesh respectively. The Lagrangian method is limited by mesh deformation and contact processing<sup>[10]</sup>. To overcome this shortage it was developed into the arbitrary Lagrangian-Eulerian method which combines advantages of the two methods. Both Lagrangian and Eulerian methods have been employed to develop various frontier flow solutions. The well-known volume of filling (VOF) method and Level Set method are interface capture methods constructed under Eulerian mesh. They have strong topological processing ability and are widely used in the simulation of front flow. In 1981, hirt et al.<sup>[11]</sup> proposed VOF method. The VOF method can be divided into an algebraic VOF method and a geometric VOF method. The geometric VOF method geometrically reconstructs the free surface, and then uses the reconstructed free surface to update the volume fraction rate distribution. The algebraic VOF method solves the volume fraction rate transport equation directly, without involving any geometric object. Existing researches show that the VOF method can depict complex interface structure and changes, and can be applied to the solution of two-phase flow<sup>[12]</sup>. Gim et al.<sup>[13]</sup> presented an improved VOF model that based on smoothing functions, which effectively reduced the issue of spurious velocities. At present, most CFD programs use variations of the VOF method to solve the interfacial problems<sup>[14]</sup>, which can be found in ANSYS Fluent, OpenFOAM, Gerris etc. Recently, Li et al.<sup>[15]</sup> developed a new calculation method via VOF method to predict the

interface evolution, velocity and the temperature distribution. Fan et al.<sup>[16]</sup> also used this approach to design a new solver called varRhoTurbVOF based on OpenFOAM software to improve the turbulence models.

Osher and Sethian<sup>[17]</sup> developed the Level Set Method is another effective approach to predict flow front evolution developed in the 1980s. This method is widely used in many disciplines such as image processing, computational geometry, optimization and computational fluid dynamics. The basic idea of this method is to express the motion of the two-phase interface with the zero point of a higher-order function (Level Set function  $\phi$ ). The value of  $\phi$  is used to distinguish the phases in the calculation area. Then update the interface by solving the advection equation of  $\phi$ . The solution of  $\phi$  may change greatly, therefore, it is necessary to reinitialize the function  $\phi$  to maintain the distance function characteristics and the accuracy of the movement of the flow front<sup>[18,19]</sup>. Sussman et al.<sup>[20]</sup> proposed a method based on partial differential equations to reinitialize the level set function in 1994. To improve the simulated precision, Dai et al.<sup>[21]</sup> proposed a piecewise constant level set method for solving the topology optimization of steady NavierStokes flow. Sodeyama et al.<sup>[22]</sup> found that the choice of re-initialization method was very important to avoid non-physical deformation of  $\phi$  and proposed a new re-initialization method to implement a multi-dimensional calculation of fluid flows. Furthermore, Hong et al.<sup>[23]</sup> established a new equidistant filling theory based on the level set function and a corresponding numerical algorithm based on the dynamic finite difference method. The algorithm can effectively produce the remanufacturing repair path of a complex die, and improve the efficiency of die manufacturing by more than 60%.

In this paper, a three-dimensional theoretical model for viscous flow driven by the vacuum is established and the finite element method is constructed to solve the flow problem. The Lagrangian method is used to track the velocity, position and shape of the jet in the early stage. When the fluid reaches the bottom, the jet flow transfers to heaping and the backward filling happens under vacuum. The new development of the flow front is simulated by the VOF method. Based on the viscous flow theory and the Lagrangian-VOF algorithm, a simulation program was developed to predict the velocity, pressure, temperature, and track the flow front and air trap position.

## 2. Vacuum Filling Theory and Numerical Method

### 2.1 Governing

The melt inertial force is much lower than the viscous

force and is neglected. The governing equations for viscous, incompressible flow are written as

$$\nabla \cdot \mathbf{u} = 0, \quad (1)$$

$$\rho \mathbf{f} - \nabla p + \nabla \cdot (\eta \dot{\gamma}) = \mathbf{0}. \quad (2)$$

Where  $\rho$ ,  $C_p$ ,  $k$  and  $\eta$  are the melt density, specific heat, thermal conductivity and viscosity respectively, and  $\rho \mathbf{f}$ ,  $\mathbf{u}$ ,  $p$  and  $\dot{\gamma} = (\nabla \mathbf{u} + \nabla \mathbf{u}^T)/2$  represent the body force, velocity, pressure and shear rate tensor respectively.

## 2.2 Boundary Conditions

The pressure are assumed to be atmosphere and vacuum at the gate and meltfront respectively

$$p = p_a \quad \text{at meltfront}, \quad (3)$$

$$p = p_v \quad \text{at meltfront}. \quad (4)$$

## 2.3 Numerical Method

Let  $\Omega_t$  denote the filled region at current time  $t$  and  $H^i(\Omega_t)$  represents the  $i$ th order Hilbert function space in region  $\Omega_t$ . Multiplying the governing equations with test functions  $(q, \mathbf{v}) \in H^1(\Omega_t) \times H^2(\Omega_t)^3$  and integrating by parts using the Gauss formula subject to the boundary conditions (3) and (4) yields the variational equations

$$\iiint_{\Omega_t} \mathbf{u} \cdot \nabla q d\Omega = \iint_{\Omega_t} \mathbf{u}_n dS \quad \forall q \in H^1(\Omega_t), \quad (5)$$

$$\iiint_{\Omega_t} \eta (\nabla \mathbf{u} + (\nabla \mathbf{u})^T) : \nabla \mathbf{v} d\Omega + \iiint_{\Omega_t} \nabla p \cdot \mathbf{v} d\Omega - \iiint_{\Omega_t} \rho \mathbf{f} \cdot \mathbf{v} d\Omega = 0. \quad (6)$$

We use the Galerkin finite element method to discretize the variational Equations (5) - (6). The part is discretized with tetrahedral elements, and the velocity  $\mathbf{u}$  is approximated with  $P_2^{(10)}$  quadratic polynomials (10 nodes) owing to their second-order derivatives in the equations. The pressure  $p$  is approximated with  $P_1^{(4)}$  linear polynomials (4 nodes). This interpolation satisfies the Brezzi-Babuska condition for numerical stability.

The pressure, velocity are interdependent in the above equations. To determine the two variables simultaneously, the time step and mesh sizes have to be satisfied the strict limitation to ensure numerical stability and convergence. Sometimes this requires a very small time step and fine mesh which involves a large number of computations. However, if the pressure is assumed to be known, then a nominal solution for velocity can be obtained from the invariant momentum Equation (6) at node  $P$ .

$$a_P^u \mathbf{u}_P + \sum_N a_N^u \mathbf{u}_N = - \sum_E c_E (\nabla p)_E. \quad (7)$$

Here  $N$  and  $E$  denote the nodes and elements surround-

ing node  $P$  respectively. Substituting this formula into the invariant continuity Equation (5) yields

$$\iiint_{\Omega_t} c \nabla p \cdot \nabla q d\Omega = Q \quad \forall q \in H^1(\Omega_t) \quad (8)$$

Equation (8) is the weak form of pseudo Poisson equation for pressure  $p$ , which makes the discrete matrix symmetric. This increases the convergence of the iterative scheme for solving linear equations, such as in the Gauss-Seidel method. When the pressure is determined the velocity can be calculated by Equation (7).

## 2.4 Fluid Advancing Simulation

The fluid used for vacuum is usually less viscous material, which leads the fluid filling like pillar flow. When the pillar arrives the bottom or contacts with the early arrived fluid, it piles along the opposite direction of gravity. The fluid advances with different manners in the two stages.

In order to trace the fluid advancement in pillar flow correctly, the Lagrange method is employed to calculate the flow fields and determine the fluid advancement. Assume a particle identified with  $\mathbf{X}$  enters the cavity, its new position can be calculated with the following formula in Lagrange expression

$$\frac{d\mathbf{X}}{dt} = \mathbf{u}. \quad (9)$$

The velocity  $\mathbf{u}$  is determined from governing equations, and the new position of the particle can be calculated with integration of Equation (9).

When the fluid switches to piled filling stage, the gravity drives the fluid to fill the remain cavity while restricted by the viscous force. The advancement is similar with viscous fluid filling droved by pressure. So the conventional volume of filling (VOF) approach is employed to predict the fluid advancement. Let  $F$  represents the filled factor of a control volume, it must satisfy the transport equation

$$\frac{\partial F}{\partial t} + \mathbf{u} \cdot \nabla F = 0. \quad (10)$$

In the first filling stage, the velocity of the particle decreases significantly once contacts with the previous arrived fluid while the viscous force increases obviously. So the velocity and viscous stress derivatives are used as the critical values switch from pillar filling to fluid advancing.

## 3. Experiment Setting

### 3.1 Experimental Equipment and Materials

The vacuum filling equipment is consisted by vacuum pump, buffer barrel, vacuum filling container and material container, see Figure 1. The buffering barrel is used to store the suction fluid to prevent backward fluid into the

pump. The experimental equipment is connected by rubber hose. The volume of the glass cup is a 300 mL, and both the suction fluid tube diameter and extraction air tube diameter are both 10 mm. Once the vacuum pump starts the fluid in the beaker will be sucked into the glass cup, and stop when the power turns off.

The flow front of the vacuum filling is recorded by video. The mixture of resin GE-7118A and curing agent GE-7114B was first used in the experiment. They are mixed at room temperature of about 20 °C, and the mass ratio of the two materials is 100:30. The vacuum filling was first performed at minus 0.75 atm and get the filling front by video, see Figure 2(a). In order to change the fluid viscosity rapidly some soil is also added to this mixture. The filling front is shown in Figure 2(b). The fluid starts accumulating along the petting pillar when the viscosity increases.

### 3.2 Improvement of Experiments

The shortage of the experiment is the flow front cannot be well captured by the camera especially for the first mixture, and the liquid column was obviously inclined. In addition, the bubbles appearing in the fluid during the experiments, which influences fluid advancing.

To improve the imagine resolution, the hair conditioner was used for experiments instead of the mixture of resin GE-7118A and curing agent GE-7114B. In order to prevent bubbles during the filling the material was drained in drying hopper at room temperature. In addition, the pipe angle was adjusted so as to the jetting column is vertical to the bottom. The flow fronts are shown in Figure 3 after improving. It can be seen that the problem of tilt jetting column had been significantly improved. The bubble and delamination phenomenon had also been removed.

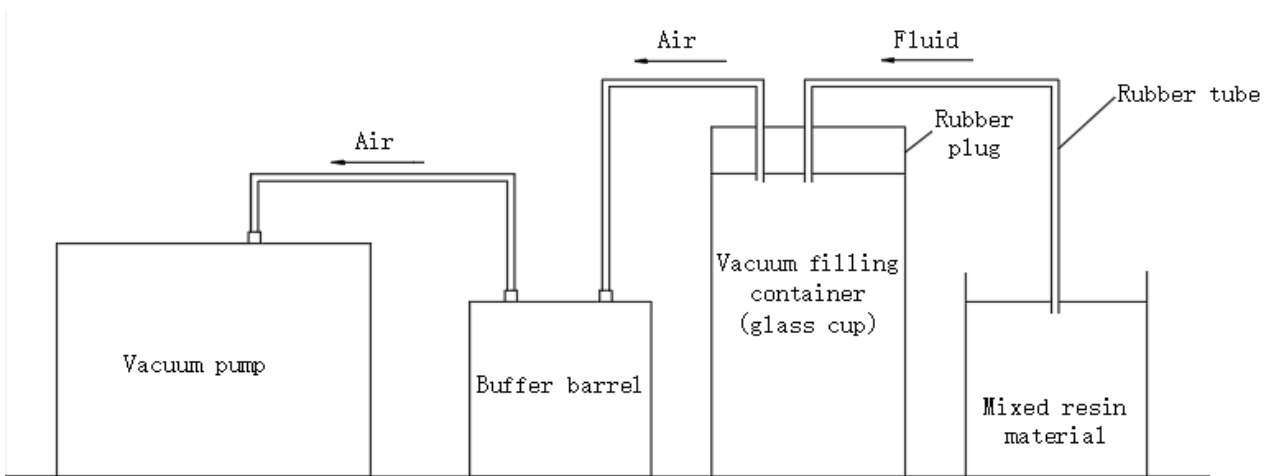


**Figure 1.** The schematic diagram of the vacuum equipment

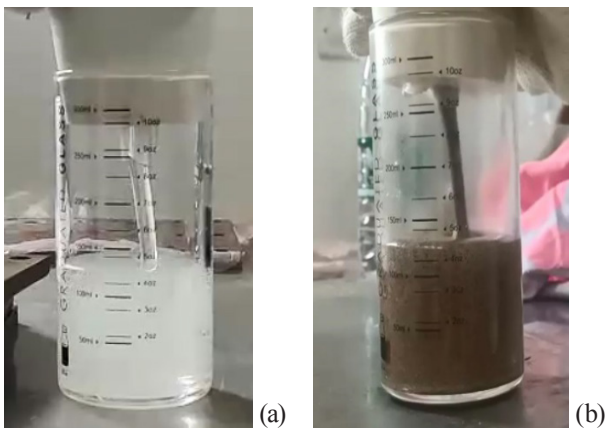


**Figure 2.** Screenshot of the vacuum filling at 1s for (a) mixture of resin and (b) mixture with additional soil.



**Figure 3.** The vacuum filling with hair conditioner.

## 4. Results and Discussion

To perform the numerical simulation, the container, see Figure 4, was discretized into 78910 tetrahedral elements. The temperature was set to ambient temperature 20 °C and the gravity direction is vertical the ground. We change the material viscosity and negative pressure to validate the proposed method.

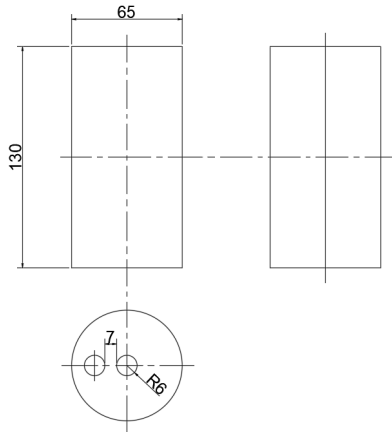


Figure 4. Schematic diagram of glass cup.

### 4.1 Viscosity Effects

The vacuum filling was firstly conducted at 1 minus atm. When the fluid enters the glass under negative pressure, it is almost equivalent to that the fluid is only affected by gravity. When the temperature does not change, the viscosity of the mixture will keep constant. The fluid does not accumulate along the jetting column and there is a slight depression near the liquid column as the viscosity is only 350 mPa·s which can not sustain the accumulated materials. We used analysis software to simulate the vacuum filling of resin mixture. The experimental and simulated fluid advancements at 1 s and 2 s are shown in Figures 5(a) and 5(b) respectively. The simulated fluid advancements are in good agreement with the experimental results. Figure 5 shows the program is also capable of simulation of the depression in low viscous vacuum.

Then some soil was added to resin to increase the material viscosity and conducted the vacuum filling again. The fluid advancements corresponding to 1 s and 2 s are shown in Figures 6(a) and 6(b). The viscosity of the sample in the experiment increases to 2500 mPa·s. The filling volume within the same period is smaller than that

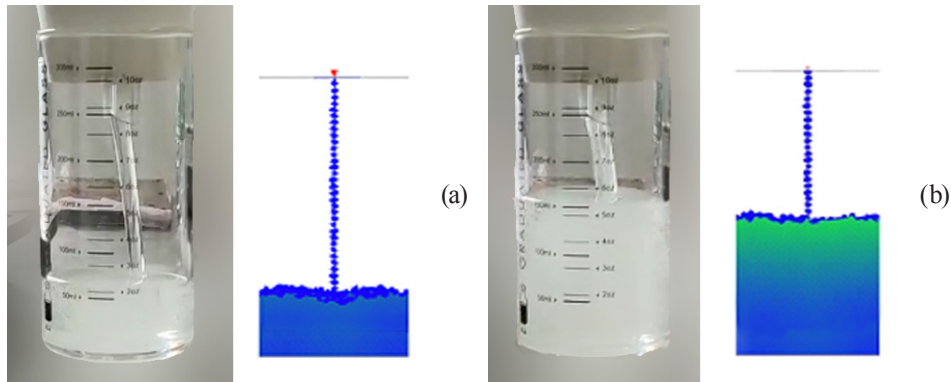


Figure 5. Comparison between experimental and simulated vacuum filling advancements at (a) 1 s and (b) 2 s under minus 1 atmosphere.

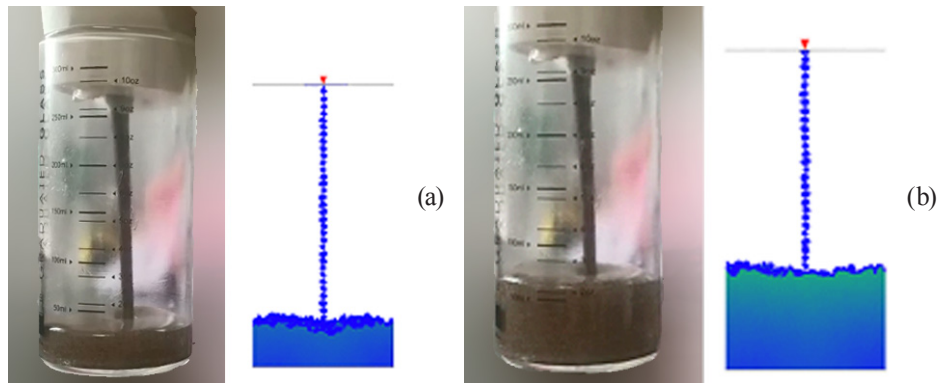


Figure 6. Comparison of experimental and simulated filling advancements of mixed resin and soil at (a) 1 s and (b) 2 s under minus 1 atmosphere

of the previous one. This is because the flow resistance increases with the enhance of fluid viscosity. Both the experimental and simulating results show that the middle depression near the liquid column still exists but shallower than before. The accumulated pyramid shape along the jetting column does not happen during the whole vacuum filling for the two materials. This mean the shape of front advancements depends on the fluid viscosity and does not change significantly for this viscosity scale.

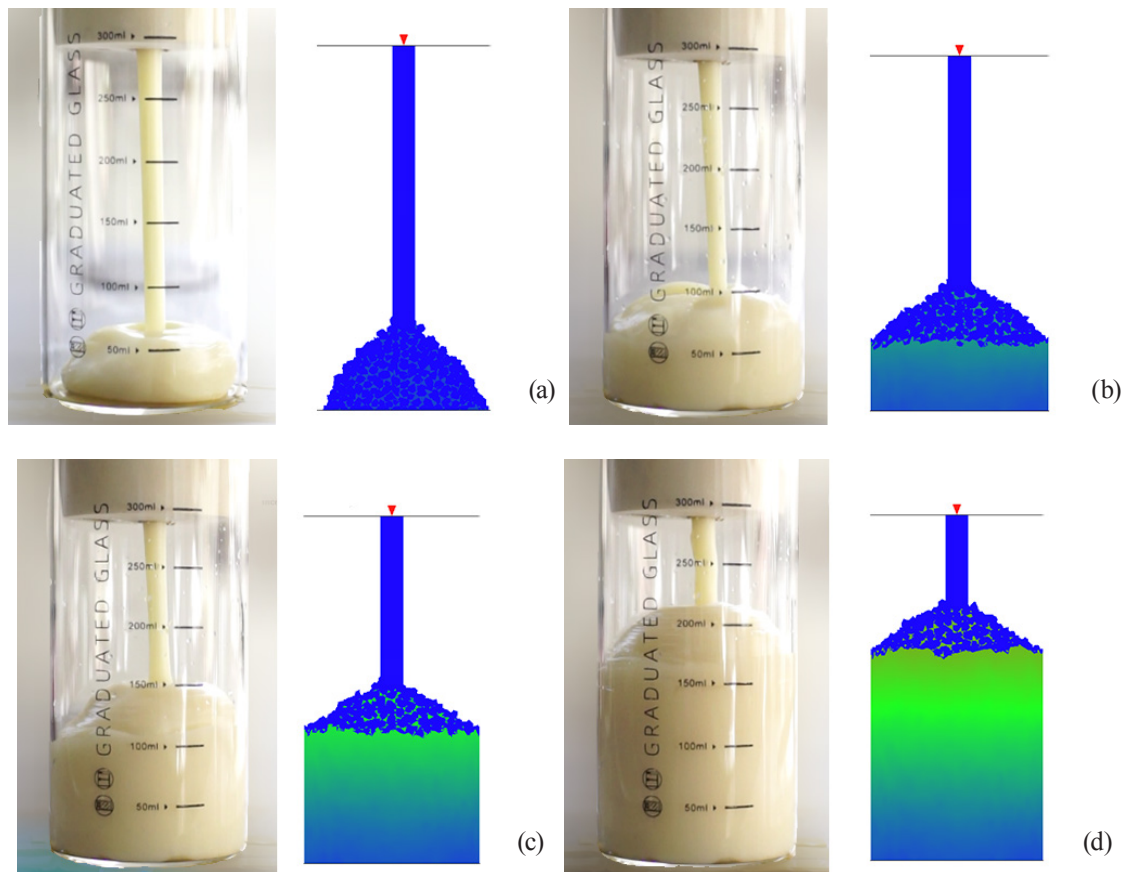
Figure 5 and Figure 6 indicate the filling speed, front shape and accumulation along the jetting pillar depend on the material viscosity. To verify this assumption, we further increased the material viscosity to 9600 mPa·s by replaced the material with hair conditioner. In addition, we have also improved the program so that the jetting column is displayed with runner elements instead of triangle elements. The experimental and simulated front advancements are shown in Figure 7.

Figure 7 shows the filled volumes are further reduced due to increased viscosity. The filling velocity is different from that of low viscosity fluid in the first stage of filling. In the initial stage of filling, it can be observed that

the time taken for high viscosity fluid to enter from the inlet to the cup of the glass increases compared with low viscosity fluid. Through the recording of the camera, we found that the low viscosity fluid took 130 millisecond. However, high viscosity fluids took 197 millisecond. In addition, the flow front shape is much different from that of low viscous fluid. The pyramid shape generates in the middle front area for high viscous fluid filling. It maintains its shape and quickly spreads around and fills the whole glass. Fortunately the developed program successfully predicts this phenomenon as we considered all the fundamental factors especially viscous force in the theoretical model. In addition, the program can predict the front heights accurately, which means the program can also work well for high viscous fluid.

#### 4.2 Negative Pressure Effects

The vacuum pressure was reduced to minus 0.75 atm. and conducted the experiment and simulation again with the soil mixture. The filling advancements corresponding to 1 s and 2 s are shown in Figures 8(a) and 8(b). The filling volumes are only half of minus 1 atm within the same



**Figure 7.** Comparison of the experimental and simulated filling front shapes for (a) 1 s, (b) 2 s, (c) 3 s and (d) 4 s under minus 1 atmosphere.

filling period. The flow front shapes are consistent with the before though the vacuum pressure changes. Meanwhile, Figure 6 and Figure 8 show the diameters of the jetting column do not vary with vacuum pressure, which indicates the jetting shape only depends on the entrance diameter and less relates the pressure.

Similarly, we also conducted comparative experiments

with high viscosity materials at the same pressure. The results are shown in Figure 9. Both experimental and simulated results illustrate that the shape of the flow front does not change much, and they are almost the same with the high vacuum one. Therefore, it once again demonstrates that the filling shape only depends on the fluid viscosity and less relate the value of vacuum which only affect the filling speed.

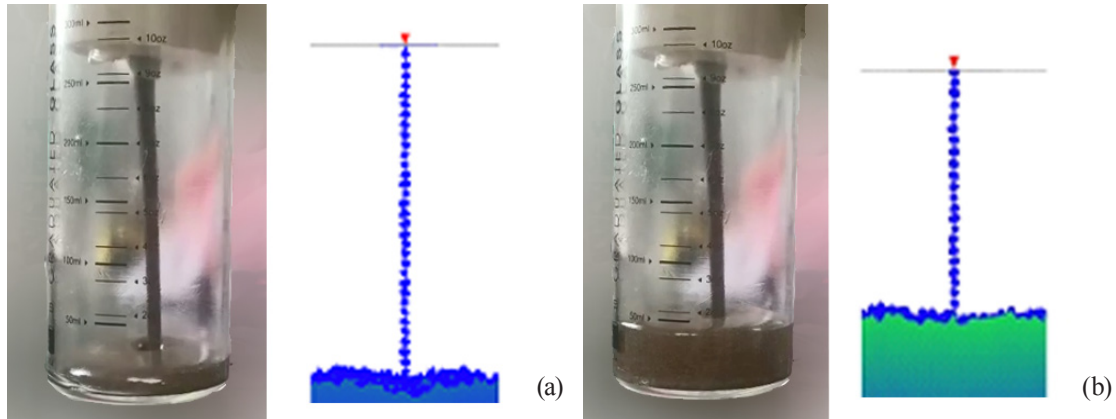


**Figure 8.** Comparison of experimental and simulated fluid advancements of mixed resin and soil at (a) 1 s and (b) 2 s under minus 0.75 atmosphere.

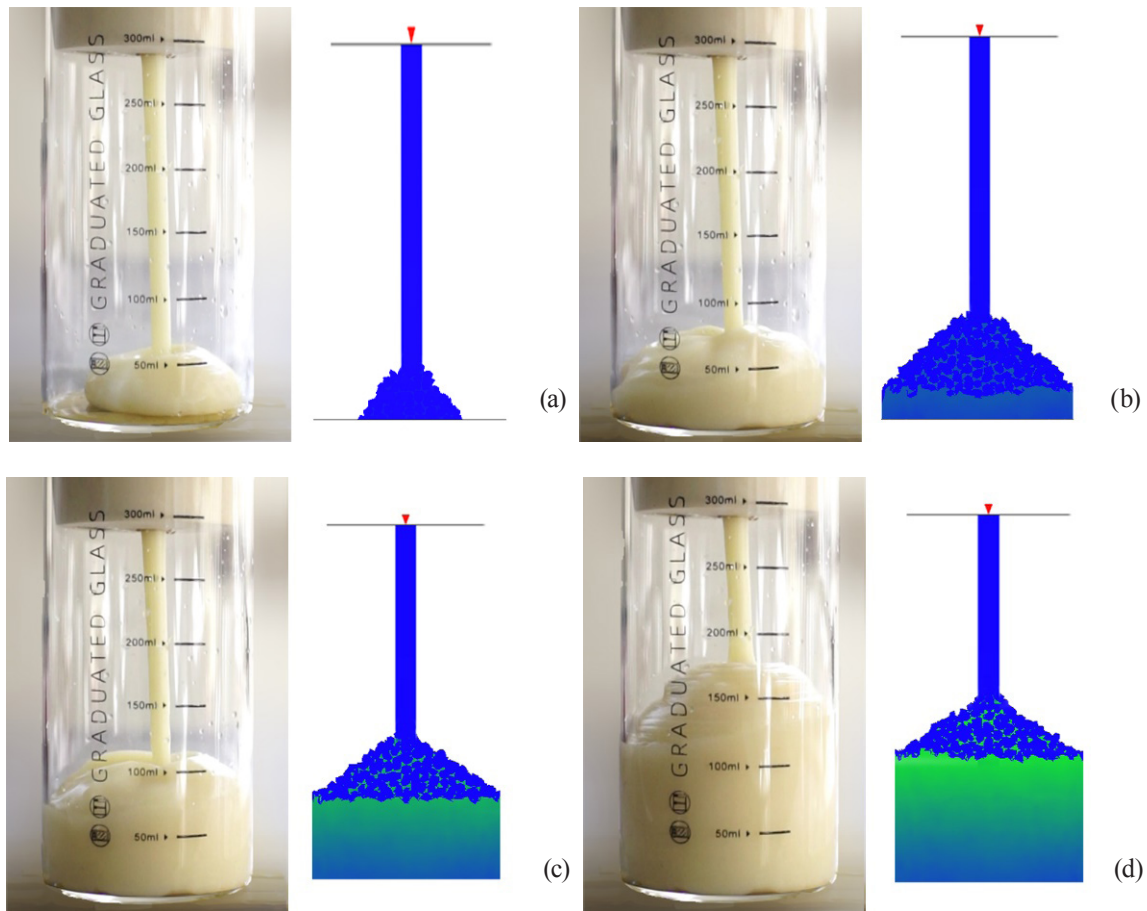


**Figure 9.** Comparison of the experimental and simulated filling front shapes for (a) 1 s, (b) 2 s, (c) 3 s and (d) 4 s under minus 0.75 atmosphere.

## 5. Conclusions

The vacuum filling is considerably different from the fluid filling of pressure-driven flow, in which the gravity force plays an important role. The conventional VOF method can not be used to simulate the flow front. In order to predict the filling process accurately a flow model is established to describe the viscous fluid. An iterative method combined with FEM is proposed to solve the flow problem. In order to capture the flow front mixed with jetting and accumulation a Lagrangian and VOF method is constructed to simulate the advancement. A series of vacuum filling experiments were conducted to validate the model and numerical methods. The results of this study show:

(a) The flow front shape closely depends on the fluid viscosity and less relates to the vacuum pressure.

(b) The depression on the middle area will be formed for the low viscous fluid vacuum filling.

(c) The pyramid front generates for high viscous fluid vacuum filling as the larger viscous material can bear heavy force.

## Acknowledgements

Financial supports from the National Science Foundation of China (No. 11672271), and Shenzhen Zhaowei Machinery & Electronics CO., LTD. (No. 20210035A and 20210035B) for this research work are gratefully acknowledged.

## Conflict of Interest

The authors do not have any possible conflicts of interest.

## References

- [1] Rodríguez-González, P., Robles Valero, P.E., Fernández-Abia, A.I., et al. (2020). Application of vacuum techniques in shell moulds produced by additive manufacturing. *Metals*. 10(8), 1-20.  
DOI: <https://doi.org/10.3390/met10081090>
- [2] Sorgato, M., Babenko, M., Lucchetta, G., et al., 2017. Investigation of the influence of vacuum venting on mould surface temperature in micro injection moulding. *International Journal of Advanced Manufacturing Technology*. 88(1-4), 547-555.  
DOI: <https://doi.org/10.1007/s00170-016-8789-8>
- [3] Xiao, L., Huang, J., Dai, Y.C., et al., 2010. Rapid fabrication of micro-gear via vacuum casting technique of silicone rubber mould. *Advanced Materials Research*. 97-101, 4016-4019. [www.scientific.net/AMR.97-101.4016](http://www.scientific.net/AMR.97-101.4016) TARGET="" \_blank">  
DOI: <https://doi.org/10.4028/www.scientific.net/AMR.97-101.4016>
- [4] Kuo, C., Liu, H., Chang, C., 2020. Optimization of vacuum casting process parameters to enhance tensile strength of components using design of experiments approach. *International Journal of Advanced Manufacturing Technology*. 106(9-10), 3775-3785.  
DOI: <https://doi.org/10.1007/s00170-019-04905-6>
- [5] Song, Y.S., Youn, J.R., 2009. Numerical investigation on flow through porous media in the post-infusion process. *Polymer Composites*. 30(8), 1125-1131.  
DOI: <https://doi.org/10.1002/pc.20668>
- [6] Robinson, M.J., Kosmatka, J.B., 2014. Analysis of the post-filling phase of the vacuum-assisted resin transfer molding process. *Journal of Composite Materials*. 48(13), 1547-1559.  
DOI: <https://doi.org/10.1177/0021998313488150>
- [7] Yang, B., Jin, T., Bi, F., et al., 2014. Modeling the resin flow and numerical simulation of the filling stage for vacuum-assisted resin infusion process. *Journal of Reinforced Plastics and Composites*. 33(21), 1976-1992.  
DOI: <https://doi.org/10.1177/0731684414551039>
- [8] Cai, Y.Q., Chen, Q.L., Zhu, Z.Y., et al., 2018. Study on VARI Process Parameters of Fiber Composites. *China Plastics Industry*. 46(07), 46-50. (in Chinese).
- [9] Shen, C.Y., Ren, M.K., Liu, C.T., et al., 2020. A review on the theories and numerical methods for injection molding simulations. *Scientia Sinica Technologica*. 50(06), 667-692. (in Chinese).
- [10] Choi, D., Lee, S., Im, Y., 2005. Fringe element reconstruction for front tracking for three-dimensional incompressible flow analysis. *International Journal for Numerical Methods in Fluids*. 48(6), 631-648.  
DOI: <https://doi.org/10.1002/fld.943>
- [11] Hirt, C.W., Nichols, B.D., 1981. Volume of fluid (VOF) method for the dynamics of free boundaries. *Journal of Computational Physics*. 39(1), 201-225.  
DOI: [https://doi.org/10.1016/0021-9991\(81\)90145-5](https://doi.org/10.1016/0021-9991(81)90145-5)
- [12] Arai, E., Villafranco, D., Grace, S., et al., 2020. Simulating bubble dynamics in a buoyant system. *International Journal for Numerical Methods in Fluids*. 92(3), 169-188.  
DOI: <https://doi.org/10.1002/fld.4778>
- [13] Soh, G.Y., Yeoh, G.H., Timchenko, V., 2016. Improved volume-of-fluid (VOF) model for predictions of velocity fields and droplet lengths in microchannels. *Flow Measurement and Instrumentation*. 51, 105-115.  
DOI: <https://doi.org/10.1016/j.flowmeasinst.2016.09.004>
- [14] Roenby, J., Bredmose, H., Jasak, H., 2016. A compu-

- tational method for sharp interface advection. *Royal Society Open Science*. 3(11), 160405-160405.  
DOI: <https://doi.org/10.1098/rsos.160405>
- [15] Li, F., Zhao, H., Ren, F., et al., 2020. Simulations and experiments of mould filling in lost foam casting. *International Journal of Cast Metals Research*. 33(4-5), 194-200.  
DOI: <https://doi.org/10.1080/13640461.2020.1822572>
- [16] Fan, W., Anglart, H., 2020. varRhoTurbVOF: A new set of volume of fluid solvers for turbulent isothermal multiphase flows in OpenFOAM. *Computer Physics Communications*. 247, 106876.  
DOI: <https://doi.org/10.1016/j.cpc.2019.106876>
- [17] Osher, S., Sethian, J.A., 1988. Fronts propagating with curvature-dependent speed: Algorithms based on hamilton-jacobi formulations. *Journal of Computational Physics*. 79(1), 12-49.  
DOI: [https://doi.org/10.1016/0021-9991\(88\)90002-2](https://doi.org/10.1016/0021-9991(88)90002-2)
- [18] Ngo, L.C., Choi, H.G., 2016. A local level set method based on a finite element method for unstructured meshes. *Journal of Mechanical Science and Technology*. 30(12), 5539-5545.  
DOI: <https://doi.org/10.1007/s12206-016-1122-5>
- [19] Ngo, L.C., Choi, H.G., 2017. Efficient direct re-initialization approach of a level set method for unstructured meshes. *Computers & Fluids*. 154, 167-183.  
DOI: <https://doi.org/10.1016/j.compfluid.2017.06.002>
- [20] Sussman, M., 1994. A level set approach for computing solutions to incompressible two-phase flow. *Journal of Computational Physics*. 114(1), 146-159.  
DOI: <https://doi.org/10.1006/jcph.1994.1155>
- [21] Dai, X., Zhang, C., Zhang, Y., et al., 2017;2018. Topology optimization of steady navier-stokes flow via a piecewise constant level set method. *Structural and Multidisciplinary Optimization*. 57(6), 2193-2203.  
DOI: <https://doi.org/10.1007/s00158-017-1850-x>
- [22] Sodeyama, K., Yoshino, H., Ohta, M., et al., 2020. Application of a level-set method for deposition of fine particles on a filter. *Kagaku Kōgaku Ronbunshū*. 46(3), 49-56.  
DOI: <https://doi.org/10.1252/kakoronbunshu.46.49>
- [23] Hong, X., Xiao, G., Zhang, Y., et al., 2021;2022. A new path planning strategy based on level set function for layered fabrication processes. *International Journal of Advanced Manufacturing Technology*. 119(1-2), 517-529.  
DOI: <https://doi.org/10.1007/s00170-021-08239-0>